LA-UR- 97-4221

CONF-9706113--

HEL-1: A DEMG BASED DEMONSTRATION OF SOLID LINER IMPLOSIONS AT 100 MA*

R.E. Reinovsky, B.G. Anderson, D.A. Clark, C.A. Ekdahl, R.J. Faehl. J.H. Goforth, I.R. Lindemuth, T.L. Petersen, P.T. Sheehey, L.J. Tabaka

Los Alamos National Laboratory, Los Alamos, New Mexico

V.K. Chernyshev, V.N. Mokhov, V.N. Buzin. O.M. Byrenkov,,, A.M. Bujko, V.V. Vakhruchev, S.F Garanin. B.E. Grinevich. Y.N. Gorbachev, E.V, Gubkov, V.A. Demidov, V.I. Dudoladov, V.V. Zmushko, A.I, Kuzyaev, A.Ik Kucherov, B.M. Lovyagin. Y.I. Matsev. P.N. Nizovtsev, A.A. Petrukhin, A.I Pishurov. S.S. Sokolov, V.P. Solovjov, A.I. Startsev, And V.B. Yakubov

All Russian Scientific Research Institute of Experimental Physics, Arzazamas-16, Sarov, Russia.

Introduction

In August 1997, the Los Alamos National Laboratory (LANL) and the All-Russian Scientific Research Institute of Experimental Physics (VNIIEF) conducted a joint experiment in Sarov, Russia to demonstrate the feasibility of applying explosive pulsed power technology to implode large scale, high velocity cylindrical liners. Kilogram mass metal liners imploding at velocities of 5-25 km/sec are useful scientific tools for producing high energy density environments, ultra high pressure shocks, and for the rapid compression of plasmas. To explore the issues associated with the design, operation and diagnosis of such implosions, VNIIEF and LANL designed and executed an practical demonstration in which a liner of approximately 1 kilogram mass was accelerated to 5-10 km/sec while undergoing a convergence of about 4:1. The scientific objectives of the experiment were three-fold. First to explore the limits of very large, explosive, pulse power system delivering about 100 MA as drivers for accelerating solid density imploding liners to kinetic energies of 25 MJ or greater. Second to evaluate the behavior of single material (aluminum) liners imploding at 5-10 km/sec velocities by comparing experimental data with 1-D and 2 D numerical simulations. Third, to evaluate the condition of the selected liner at radial convergence of 4 and a final radius of 6 cm. A liner of such parameters could be used as a driver for equation of state measurements at megabar pressures or as a driver for a future experiment in which a magnetized fusion plasma would be compressed to approach ignition conditions.

Pulse Power and Liner System

The pulse power system selected to drive the liner is shown in Figure 1. A 5 module Disk Explosive Magnetic Generator (DEMG) whose diameter is 1000 mm provides the 100 MA driving current. As discussed elsewhere in this conference (1),(2), the DEMG is an, explosively powered magnetic flux compression generator capable of delivering several hundred megamperes of current to low inductance loads in time-scales of 25-50 μs. The disk shaped explosive charges are initiated on the cylindrical axis and the detonation front moves radially outward. Relatively thin metal conductors forming the walls of the flux compression cavities surround the explosive charges. The detonating high explosive accelerates the metal walls (primarily) in the axial direction compressing the cavities first near the axis and subsequently at progressively larger radii "pushing' the magnetic flux outward to the high current

* Work Supported by US Department of Energy

DISCLAIMER

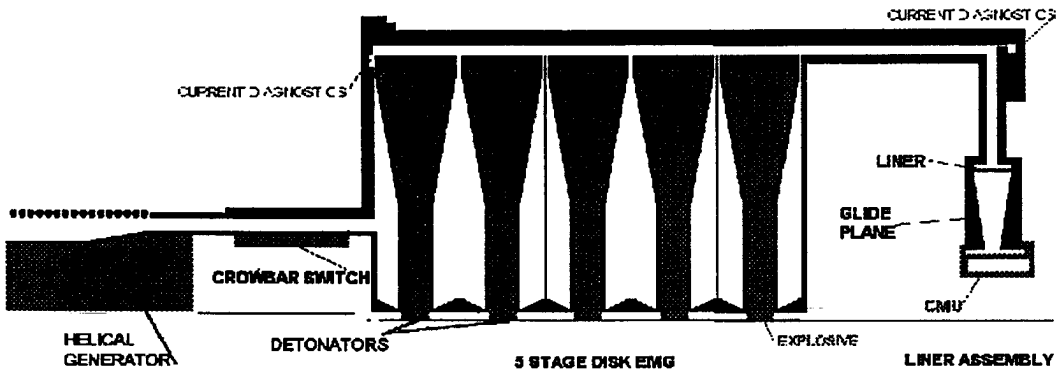

Figure 1: System configuration for HEL-1

coaxial transmission lines and ultimately into the liner load. As shown in the figure, the cavities are connected in series, making it possible to drive higher inductance loads by adding modules to the system. For the experiment reported here, 5 modules were used each with an initial inductance of about 24.07 nH. A helical flux compression generator provides initial current for the DEMG, and a modest capacitor bank coupled to the helical generator through a multi-turn inductive coupling coil coaxial transmission lines and ultimately into the liner load. As shown in the figure the cavities are supplies initial flux for the helical generator. The helical generator supplied 9.1 MA to the five stage disk generator, and the disk generator produced a 102 ± 2.5 MA current pulse to drive the liner load.

The liner was initially a right circular cylinder, 240 mm in radius, 100 mm tall and 4 mm thick (± 10 □) made from a high strength aluminum alloy (6% Magnesium) designated as AMg-6 in Russia and similar to Al 6061 in the US. The liner was fabricated to a surface finish of about 0.32 microns on the outside and 0.63 microns on the inside. The active part of the liner had a total mass of about 977 grams. Special attention was directed to the current joints connecting the liner to the transmission line structure and to the steel glide-planes that bounded the ends of the liner during implosions. The glides planes sloped inward at an angle of 8° in order to insure that god electrical contact was maintained between liner and wall.

The liner was mechanically isolated from the DEMG by a coaxial transmission line 500 mm in radius and about 600 mm in length. A radial transmission line segment was connected to the coaxial line delivering current to the 240-mm liner. The transmission line was solid dielectric insulated throughout using a Russian produced polyester sheet material similar to mylar. The initial loading of the helical generator from the capacitor bank took 355 μs. The operating time for the helical generator was about 162 μs. Final DEMG operating time was about 53 μs, and the liner implosion time after peak current was about 27 μs. Thus the entire duration of the experiment was approximately 600 μs.

Pulse Power System Performance

Current in the pulse power system was measured at several locations using inductive magnetic probes configured as local B-dot probes and as Rogowski belts. In addition, current at the connection between coaxial and radial transmission line and the, nominally identical, current delivered to the liner load was measured with optical Faraday effect current diagnostics employing rotation of polarized 829 nm laser light in a quartz fiber. Careful evaluation of the Verdet constant of the fiber, plus detailed knowledge of the measuring geometry provides very accurate evaluation of large currents without making electrical connection to the system. The rotation is measured with an optical polarization analyzer and recorded as intensity fringes on transient recorders. With a basic sensitivity of 1.24 MA/fringe and a quadrature detection system, this diagnostic is convenient for currents from one to several hundred MA and is complementary with inductive magnetic current measurements. Inductive probes suffer from the effects

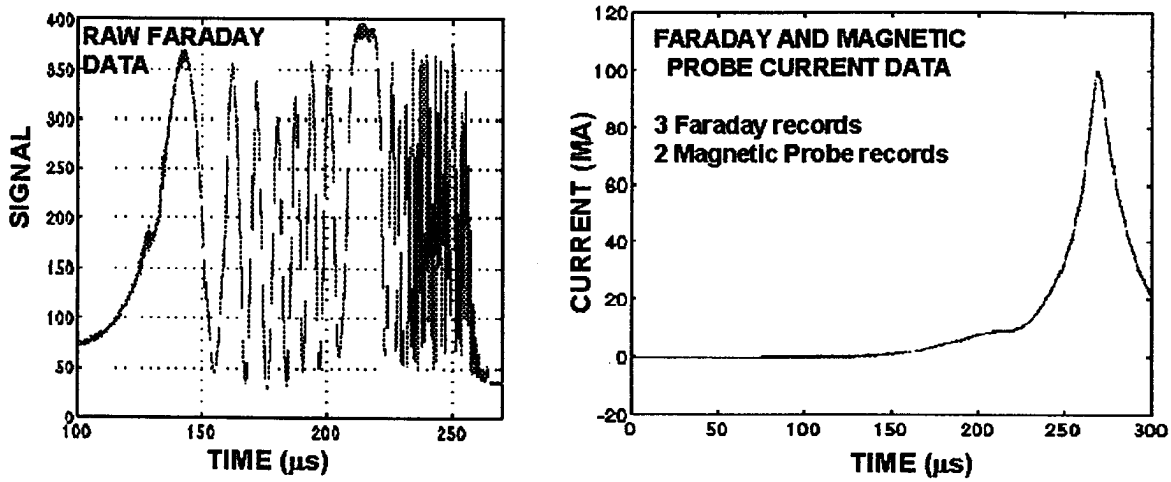

Figure 2 Current Measurement by faraday rotation and inductive probes

of tiny baseline uncertainty in recording of dI/dt. When integrated for long times, these small uncertainties can result in significant uncertainties in the determination of peak currents. On the other hand the optical fiber in the Faraday diagnostic is subject to mechanical damage and to the effects of bi-refringence in the material. This was forcefully illustrated in the present experiments where the optical fibers suffered mechanical damage a few microseconds before peak current. Figure 2 shows comparison of Faraday with inductive measurements of the system current. Faraday measurement provided absolute corrections for baseline uncertainty in the inductive probe measurements and the inductive probes provided recording for the full duration of the experiments

Phenomenological models of DEMG operation have been developed (2) and are the source of design information for planning applications experiments. At the measured peak current of 100 MA, the pulse power system delivered about 20% less current than anticipated in a nominal prediction of system performance. The decrease in the value of current at peak can be explained in circuit modeling by the addition of approximately 3.4 nH to the nominal 3 nH transmission line inductance. Alternatively, the addition of about 0.13 mΩ provided a reasonable match to peak system current. The comparison of model and measured current is shown in Figure 3. Conceptually, additional transmission line inductance can be attributed to motion of the transmission line conductors caused by the magnetic pressure resulting from the large currents. Similarly, additional resistive losses can be conceptually attributed to *poor contact appearing in current joints in the transmission lines. Local resistive losses at current joints*

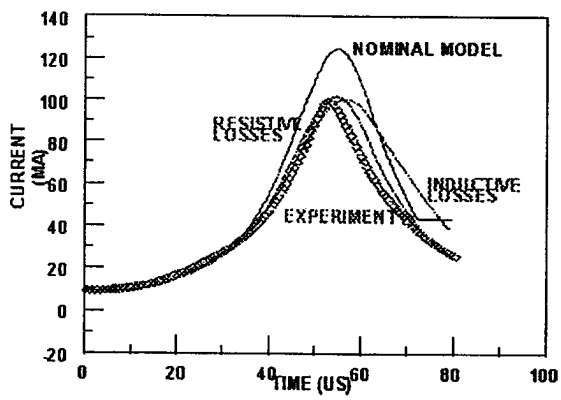

Figure 3 Circuit models of system performance

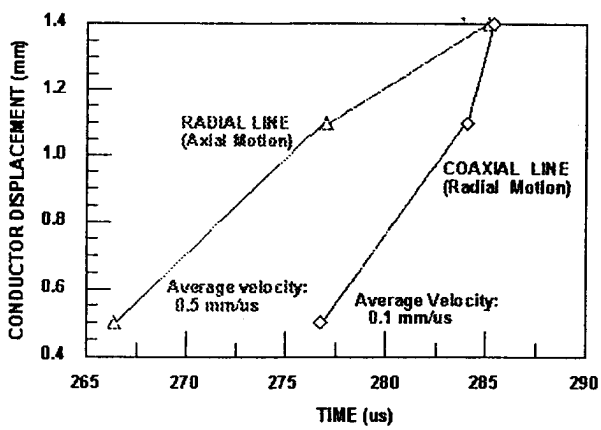

Figure 4 Motion of transmission line conductors

would be expected to give rise to voltage drops across the joints that would be observable from outside the line. Conductor motion could likewise be observed from outside the transmission line structure. As part of assessing the performance of the pulse power system, voltage measurements were made using resistive voltage dividers located across current joint in two locations – one at the corner where the coaxial line joins the radial line and the second as near a practical to the liner load. The voltage measurements, sensitive to about 100 volts, found no detectable voltage which implied no significant flux losses at these locations.. Two arrays of contact probes were also fielded to assess motion of transmission line conductors during the current pulse. Prior to the experiment analytic estimates of axial and radial motion were made. As shown in Figure 4, one array of probes was located to measure the radial motion of the outer conductor of the coaxial transmission line and one array was located to measure the axial motion of the radial transmission line. The figure shows the time dependent motion at the two locations. In both cases the measured motion corresponded closely to the pre-shot analytic estimates. The outer wall of the coaxial line moved at about 0.1 mm/us and added about 1.6 nH to the system inductance by the end of the experiment. Near the liner the radial line reached a velocity of about 0.5 mm/us and added another 1.6 nH to the system inductance. Thus the total 3.2 nH additional inductance is remarkable close to the for the 3.4 nH needed to explain the 20 % decrease in peak current.

Liner Performance

The first step in assessing liner implosion is to evaluate bulk liner motion. Voltage measured across the transmission line immediately outside the liner is a diagnostic of the flux delivered past the measuring location to the load. With a precision measurement of current from optical and inductive probes, voltage data can be analyzed to arrive at the time dependent inductance (radius) of the average current radius (presumably the back surface of the liner). A voltage measurement was made using capacitive probe operated into a 50 Ω terminated cable to record dV/dt. When integrated numerically, the peak measured voltage was about 17 kV. Figure 5 shows the trajectory in R-T space implied by the voltage measurement compared with a 1-D MHD calculation of liner position. The calculation was driven by the experimentally measured current profile. . When interpreted directly, the trajectory inferred from the voltage measurement appears to lag (that is imply a larger radius at a given time) compared to the trajectory predicted by the MHD calculation by about 20 mm. However, Figure 4 shows that the transmission lines moves 1-2 mm during the course of the experiment and since this motion decreases the coupling to the capacitive probe, such motion would result in decreased signal on the recorder.

This signal would in turn be interpreted as an erroneously low voltage and an erroneously low flux delivery to the load – or in other words to an erroneously large implied liner radius. Using the information in Figure 4, a time dependent correction was applied to the probe sensitivity and Figure 5 shows the result of the measurement after the correction. The effective electrical radius of the current in the liner still appears lag the predicted location of the liner mass at early times in the experiments, but appears to

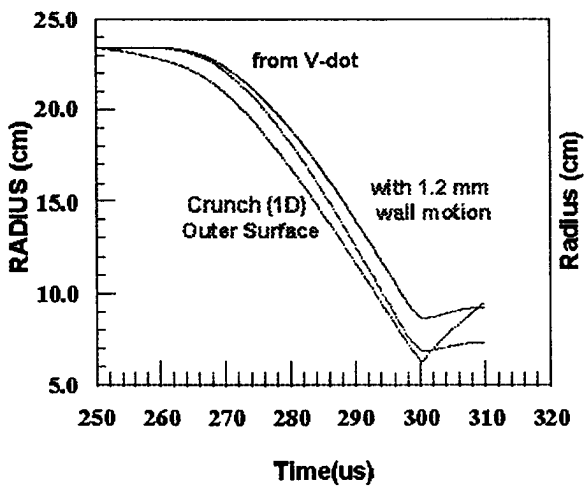

Figure 5 Implosion trajectory from voltage

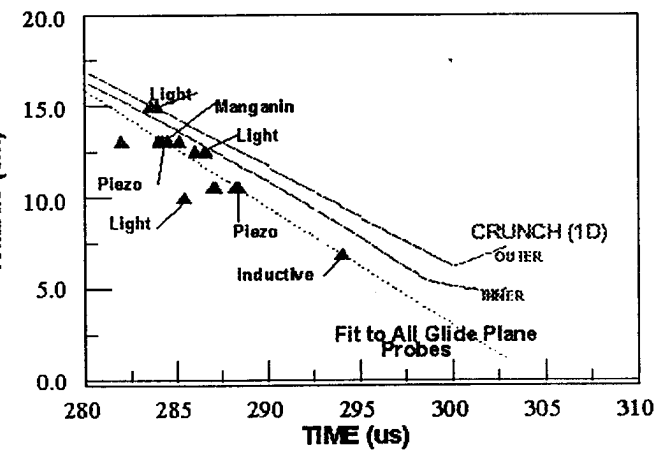

Figure 6 Glide plane diagnostics

catch up to the predicted liner location as the experiment proceeds. One interpretation of these data is that the ohmic heating on the back surface of the liner thermally liberates a small amount of gas, water vapor or insulator material from the polyethylene insulator during the long rise of the main discharge current. As the liner begins to move, the vapor expands drops in density and electrical break-down occurs allowing some of the current to remain on the insulator surface for some time. As the current increases, both boiled-off vapor and liner are accelerated inward and ultimately the vapor is collected and compressed against the back surface of the liner carrying the current along with it. Since the liner is no longer in contact with the insulator, gas production is reduced and the average current radius is near the 1-D prediction at the end of the experiment.

To further track the liner's implosion, an array of probes were located in the glide planes to monitor time of the liners arrival at several radii. Figure 6 shows a composite plot of arrival time from the array of probes which included optical (beam interruption) probes, Maganin pressure probes, piezo-electric pressure probes and inductive probes. In all cases the probes were located at the surface of, or recessed into the glide planes. The plot also includes the predicted location of the inner and outer surface of the liner from a 1-D prediction. In general, the probes are seen to imply that at least the part of the liner in contact with the electrodes arrived at a given radius earlier than the predicted arrival time The figure shows a linear fit to all glide plane diagnostics and taken together, the glide plane probes indicate a liner velocity at the electrodes of about 6.6 km/sec and leading the 1-D trajectory by 1-1.5 cm or 2-2.5 ms.

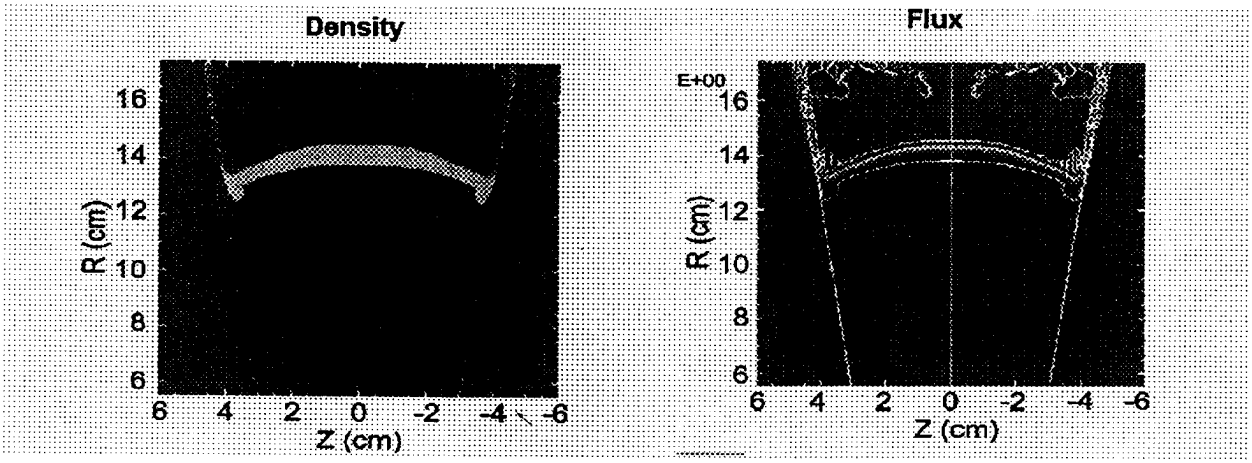

Figure 7 Two dimensional calculations showing liner bowing and glide plane run ahead

Two-dimensional calculations were conducted to assess the detailed shape of the liner during implosion, Figure 7 shows the results from one of those calculations when the liner has reached about 12 cm radius(halfway through the implosion). Additional details of the 2-D calculations can be found in a companion paper in this conference (3). The figure shows contours of density and the contours of magnetic flux – essentially identifying the location of the current. The flux plot shows that current is being carried in the outer 1/3 of the liner mass. This is significant because it suggests that the inner surface of the liner is unaffected by ohmic heating and hence retains much of its nominal strength. The fact that the inner surface of the liner is near room temperature is also directly confirmed by both 1-D and 2-D calculations. As the liner passes the radial location of the glide plane probes, the edges of the liner appear to lead the material in the center of the liner. As the liner is imploded between the axially converging glide planes, the motion would be expected to introduce substantial axial loading on the liner. Since the liner retains a significant amount of its initial strength, the application of significant axial pressure, would be expected to distort the liner in a manner similar to buckling in a loaded column. Furthermore, the flux plot shows concentration of field (current) at the contact point between liner and wall. This would be expected to result in increased heating at the glide plane, loss of strength and preferential acceleration of liner material near the glide plane as the magnetic field seeks to push through the liner at its weakest point. Thus the 2-D calculated results are consistent with the early arrival of material at the glide plane detectors.

In addition to the glide plane diagnostics, an array of contact pins was employed to measure the arrival of the liner at the radius of a central measuring unity located at radius of 55 mm. The diagnostics in the CMU included optical, electrical time of arrival probes, manganin pressure probes and inductive probes. Detailed results of these measurements are presented in a companion paper (4). Figure 8 shows time of arrival of the liner measured by an a subset of the array of probes in the CMU. This subset is arranged to measure the axial unformity of the liner's arrival. The plot shows that the line material at the glide plane arrives at the CMU about 2 μs earlier than does the material in the midplane of the liner. This is again consistent with the results predicted by the 2-D calculations.

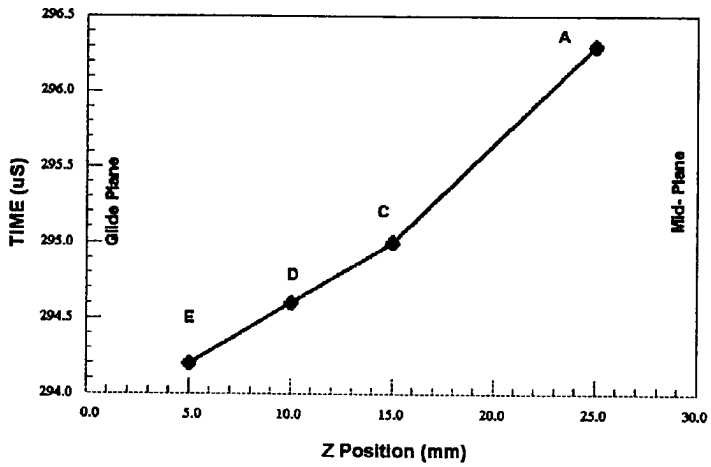

Figure 8 Time of arrival at CMU probes

Results

The DEMG system delivered current and energy to the imploding liner well within the expected parameters. Losses resulting from flux losses, for example at the current joints in the generator was minimal. Conductor motion in the transmission lines was observed and quantitatively confirmed to be close to that anticipated from simple analytical models. 1-D models accurately predicted the general behavior of the liner dynamics. With more than 50% of the liner mass unmelted, 2-D effects were manifested (computationally) in "glide plane run-ahead.". Experimental measurements were consistent with these predictions. Liner velocity at the CMU was between 6.7 and 8.4 km/sec. Liner kinetic energy at the CMU (4:1 radial convergence) was between 22 and 35 MJ. In general, the experiment demonstrated the feasibility of accelerating kilogram mass liners to velocities above 5 km/sec using explosive pulse power systems, but suggested that significant work remains to be done to address the detailed shape and uniformity of the liner before practical applications can be envisioned,

References

1) "Study of Condensed High_Energy Liner Compression in HEL-1 Experiment", V.K. Chernyshev et al. Proceedings of the 11 IEEE International Pulse Power Converence, Baltimore Md, July 1997.
2) "Caballero: A high Current Flux Compressor Based on a Disk Configuration, R.E. Reinovsky, I.R. Lindemuth, E.A. Lopez, J.H. Goforth, S.P. Marsh, Proceedings of the 11 IEEE International Pulse Power Converence, Baltimore Md, July 1997.
3) "Modeling and Analysis of the High Energy Liner Experiment, HEL-1, R.J.Faehl, P.T. Sheehey, R.E. Reinovsky, I.R. Lindemuth, A.M. Buyko, V.K. Chernyshev, S.F. Garanin, V.N. Mokhov, V.B. Yakubov, Proceedings of the 11 IEEE International Pulse Power Converence, Baltimore Md, July 1997.
4) "High Energy Imploding Liner Experiments HEL-1:Experimental Results, D.A Clark et al. Proceedings of the 11 IEEE International Pulse Power Converence, Baltimore Md, July 1997.

Report Number (14) LA-UR--97-4221
CONF-9706113--

Publ. Date (11) 199712
Sponsor Code (18) DOE/DP, XF
JC Category (19) UC-700, DOE/ER

DOE